Corrosion control of carbon steel in phosphoric acid by 6-methyl-7H-1,2,4-triazolo[4,3-b][1,2,4]-triazepine-8(9H)-thione: Electrochemical studies

Y. El Bakri[1]*, Y. El Aoufir[2,3], H. Bourazmi[2], A. Harmaoui[1], J. Sebhaoui[1],
M. Tabyaoui[2], A. Guenbour[2], H. Oudda[3], H. Lgaz[3,5], F. El Hajjaji[6], A. Ben Ali[2],
Y. Ramli[4] and E.M Essassi[1]

[1]*Laboratoire de Chimie Organique Heterocyclique, URAC 21, Pôle de Compétences Pharmacochimie, Universite Mohammed V, Faculte des Sciences, Av. IbnBattouta, BP 1014 Rabat, Morocco.*
[2]*Materials, Nanotechnology and Environment Laboratory, Faculty of Sciences, Mohammed V University Rabat, Morocco.*
[3]*Separation Processes Laboratory, Central Post, Kenitra, Department of Chemistry, Faculty of Sciences, University Ibn Tofail, Morocco.*
[4]*Medicinal Chemistry Laboratory, Faculty of Medicine and Pharmacy, Mohammed V University, 10170 Rabat, Morocco.*
[5]*Laboratory of Applied Chemistry and Environment, ENSA, Ibn Zohr University, PO Box 1136, 80000 Agadir, Morocco*
[6]*Laboratoire d'Ingénierie d'Electrochimie, Modélisation et d'Environnement (LIEME), Faculté des sciences, Université Sidi Mohammed Ben Abdellah, Fès, Maroc.*

Abstract

The corrosion inhibition properties of 6-methyl-7H[1,2,4]triazolo[4,3-b][1,2,4] triazipine-8(9H)-thione (MTTT) on carbon steel in phosphoric acid (2M H3PO4) solution has been examined and characterized by Tafel polarization and electrochemical impedance spectroscopy (EIS) methods. The experimental results reveal that the compound has a good inhibiting effect onthe carbon steel in 2 M H3PO4 solution. The protection efficiency increases with increasing inhibitor concentration, but the temperature has hardly effect on the inhibition efficiency of MTTT. The adsorption of this compound is found to obey the Langmuir adsorption isotherm. Potentiodynamic polarization studies have shown that MTTT acts as a mixed type of inhibitor. Data obtained from EIS studies were analyzed to model inhibition process through appropriate equivalent circuit model(ECM).

1. Introduction

The corrosion of metals is the most serious problem in some fields industrial, such as: oil production, oil refining, chemical and petrochemical manufacture, fertilizer production, power stations, and civil engineering structures involving buildings and bridges [1]. Generally, Acid solutions are widely used for removal of undesirable scale and rust in metal working, cleaning of boilers and heat exchangers, oil-well acidizing in oil recovery [2–4]. Phosphoric acid is widely used in the production of fertilizers and surface treatment of steel

such as chemical and electrolytic polishing or etching, chemical coloring, removal of oxide film, phosphating, passivating, and surface cleaning, also most of the acid is produced from phosphate rocks. Knowing that, ferrous alloys (or steel) are readily corroded during these applications [5]. The use of organic inhibitors for decrease the corrosion rate is a more favorable and effective solution. All Organic compounds containing heteroatoms with high electron density such as oxygen, nitrogen, sulphur, phosphorus, unsaturated bonds or plane conjugated systems are more effective as corrosion inhibitor [7-10]. In general, the organic inhibitors act by adsorption for blocking the active sites of the metal surface through displacing water molecules and forming a compact barrier film to decrease the corrosion rate. Accordingly, the aim of this work is to study the inhibition action of 6-methyl-7H-[1,2,4]triazolo[4,3-b][1,2,4]triazepine-8(9H)-thione (MTTT), on the corrosion of carbon steel in phosphoric acid. The inhibition performance is evaluated by electrochemical impedance spectroscopy (EIS) and potentiodynamic polarization measurements. The chemical structure of MTTT is given in Fig. 1.

2. Experimental methods

2.1. Materials

The steel used in this study is a carbon steel (CS) (Euronorm: C35E carbon steel and US specification: SAE 1035) with a chemical composition (in wt%) of 0.370% C, 0.230% Si, 0.680% Mn, 0.016% S, 0.077% Cr, 0.011% Ti, 0.059% Ni, 0.009% Co, 0.160% Cu and the rest being iron (Fe).

2.2. Solutions

The aggressive solutions of 2M H_3PO_4 was prepared by dilution of analytical grade 85% H_3PO_4 with distilled water. The concentration ranges of (MTTT) employed was 10^{-6}–10^{-3}M.

2.3. Inhibitor

Triazolotriazepine derivatives have been used as potent inhibitors of bone resorption (Chikazu et al., 2000). They also exhibit anti-fungal activity (Gupta et al., 2011) [15]. These compounds have been synthesized in view of the potential biological activity of fused azepines (Dabholkar & More, 2004; Sewell & Hawking, 1950; Acheson & Taylor, 1956) and as part of our interest in the synthesis of new heterocyclic systems containing triazole and triazepine rings (Essassi et al., 1976, 1977; Gupta, 2007) [11-16].
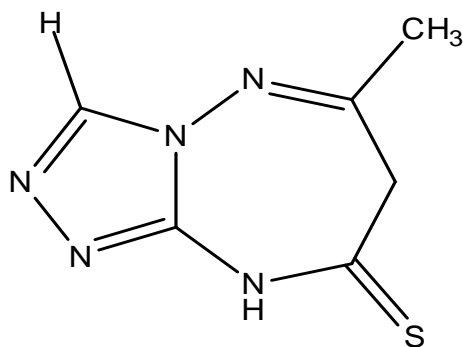
Figure 1: The molecular structure of 6-methyl-7H-1,2,4-triazolo[4,3b][1,2,4]-triazepine-8(9H)-thione (MTTT).

Synthesis of 6-methyl-7H-1,2,4-triazolo[4,3-b][1,2,4]triazepine-8(9H)-thione

To a solution of 6-methyl-7H-1,2,4-triazolo[4,3-b]-[1,2,4]-triazepin-8(9H)-one and 2.2g pentasulfide in 40ml of acetonitrile, to which was added a pinch of sodium bicarbonate was heated at gentle reflux for 4 hours then evaporated to dryness, the residue is taken up in 20 ml of boiling water, the precipitate formed by cooling was filtered. The purified product was crystallized from ethanol to give colourless crystals with a yield of 65% (Scheme 1)

(i) : CH₃CN, NaHCO₃, Δ, 4h
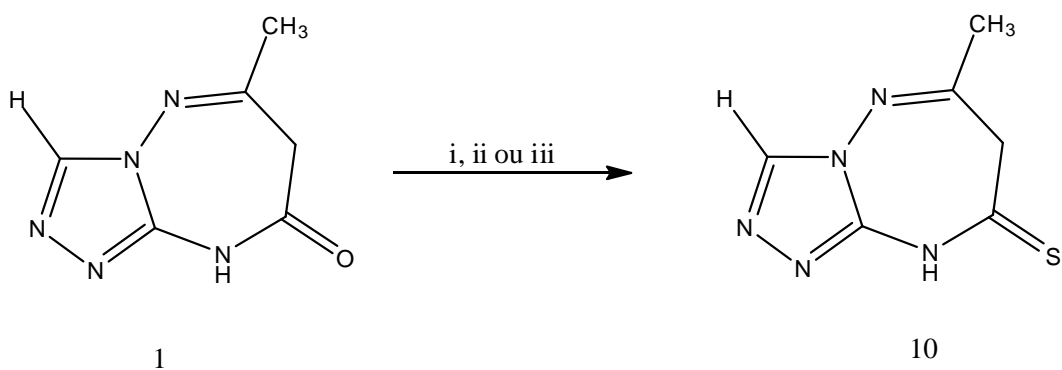
(i) : CH_3CN, $NaHCO_3$, Δ, 4h
(ii) : P_2S_5, Pyridine, Δ, 4h
(iii) : Lawessen reagent, Toluene, Δ, 24h

Scheme1: Synthesis of 6-methyl-7H-1,2,4-triazolo[4,3b][1,2,4]triazepine-8(9H)-thione

The compound was characterized by N.M.R. ^{1}H-NMR (DMSO-d6) (δ ppm): 2.27(s,3H,CH₃), 3.98(s,2H,CH₂), 8.83(s,1H;H$_{triazolique}$). ^{13}C-NMR(DMSO-d6) (δ ppm): 24.34(C-CH₃), 51.90(C-CH₂), 141.70(C$_{triazolique}$), 141.705(C=S).

2.4. Measurements

2.4.1. Electrochemical impedance spectroscopy

The electrochemical measurements were determined experimentally out using a Volta laboratory (Tacussel-Radiometer PGZ 100) potentiostate and controlled by Tacussel corrosion analysis software model (Volta-master 4) at under static condition. The corrosion cell used had three electrodes. The reference electrode was a saturated calomel electrode (SCE). A platinum electrode was used as an auxiliary electrode of surface area 1 cm². The working electrode was carbon steel with the surface area of 1 cm². All potentials given in this study were referred to this reference electrode. For each experiment, the working electrode was immersed in test solution for 30 min to establish a steady state open circuit potential (E$_{ocp}$). After measuring the E$_{ocp}$, the electrochemical measurements were performed. All these measurements were done at 303 K.The EIS measures were determined in the frequency range between 100 kHz et 0.1 Hz at open circuit potential, with 10 points per decade, at the rest potential, after 30 min of immersion, by applying 10 mV ac voltage peak- to-peak.The inhibition efficiency of the inhibitor was calculated from the charge transfer resistance values using the following equation [17]:

$$\eta_Z \% = \frac{R_{ct}^i - R_{ct}^\circ}{R_{ct}^i} \times 100 \qquad (1)$$

where, R_{ct}° and R_{ct}^i are the charge transfer resistance in absence and in presence of inhibitor, respectively.

2.4.2. Potentiodynamic polarization

The electrochemical behavior of carbon steel sample in inhibited and uninhibited solution was studied by recording potentiodynamic polarization curves. Measurements were performed in the 2M H₃PO₄ solution containing different concentrations of the tested inhibitor at the potential range of -900 to +100 mV (SCE) and scan rate of 1 mV /s.

The inhibition efficiency ($\eta_{Taf} \%$) was evaluated from the measured I$_{corr}$ values using the relationship:

$$\eta_{Taf} \% = \frac{I_{corr}^\circ - I_{corr}^i}{I_{corr}^\circ} \times 100 \qquad (2)$$

Where I_{corr}° and I_{corr}^i are the corrosion current density in absence and presence of inhibitor, respectively.

2. Results and discussion

2.1. Potentiodynamic polarization measurements

Tafel polarization curves for carbon steel corrosion in 2M H_3PO_4 in the absence and the presence of different concentration of MTTT at 303 K are   presented in figure2.These curves show that the values of inhibitor decrease significantly with the increase of inhibitor concentration, and retard the electrochemical reaction by formation of protective film on metal surface. it can also be observed that both cathodic and anodic reactions presents in figure were affected in the presence of MTTT, also the cathodic reactions are more affected than anodic reactions with low variation in E_{corr} values (<85 mV) suggesting that MTTT are mixed type but predominantly cathodic inhibitors [18].
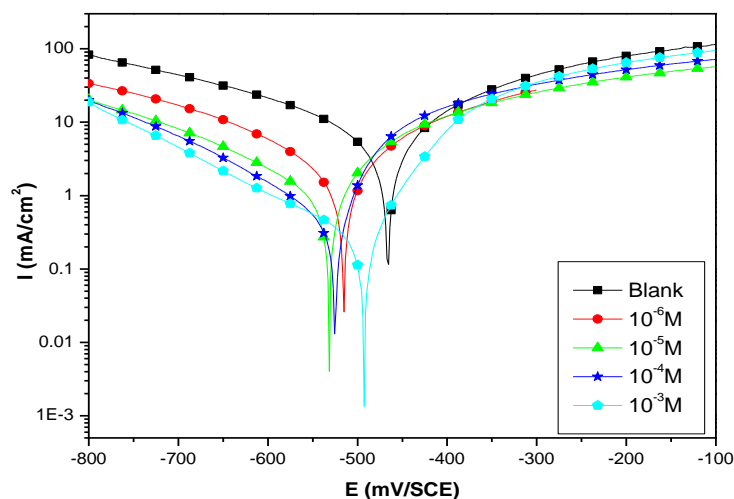
Figure 2: Potentiodynamic polarization curves of carbon steel in 2M H_3PO_4 in the presence of different concentrations of MTTT at 303K.

Table 1: Polarization parameters and the corresponding inhibition efficiency of carbon steelcorrosion in 2 M H_3PO_4 containing different concentrations of MTTT at 303 K.

Concentration(M)	E_{corr}(mVvs.SCE)	I_{corr} ($\mu A\ cm^{-2}$)	$-\beta_c$ ($mV.dec^{-1}$)	η_{Tafel}(%)
Blank	-470	3405	193	-
10^{-6}	-519	1348	128	60.41
10^{-5}	-536	660	122	80.61
10^{-4}	-528	352	111	89.66
10^{-3}	-496	271	179	92.04

2.2. EIS measurements

Fig 3 represents the typical Nyquist in the absence and the presence of different concentration of the MTTT. The EIS parameters namely solution resistance (R_s), charge transfer resistance (R_{ct}), CPE constant(Q), surface inhomogeneities (n), double layer capacitance (C_{dl}), and inhibition efficiency (η_{EIS}),were determined according to equivalent circuit (Fig 4) and given intable2.

The equivalent circuit is composed of R_s the solution resistance, CPE the constant phase element, R_1 the polarization resistance, L the inductance, and $R_1 + R_2$ presents the charge transferresistance (R_{ct}). Resistance R_2 and inductivity L may be correlated with a slow low frequency intermediate process [19]. The Nyquist diagram in Fig. 3, obtained for carbon steel without and with addition of MTTT, are characterized by one capacitive loop at high frequency (HF) with small inductive one at low-frequency (LF) values. The capacitive loop appearing at HF region can be attributed to the charge transfer, while the inductive one at LF region is relates to the relaxation process of the adsorbed intermediates controlling the anodic process [20].
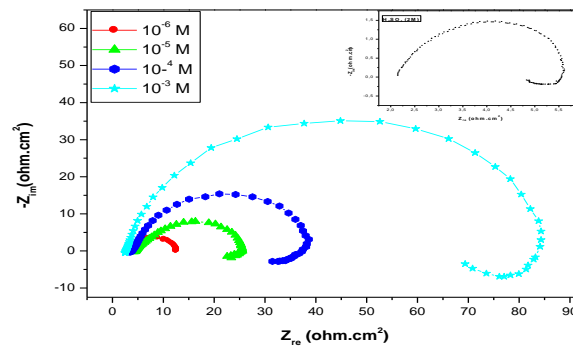
Figure3: Nyquist diagrams for carbon steel in 2M H_3PO_4 containing different concentrations of MTTT at 303K.
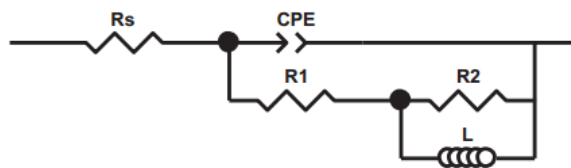
Figure 4: Equivalent circuit model for the carbon steel/phosphoric acid electrolyte.

Indeed, the inductive behavior is probably due to the consequence of the layer stabilization by products of the corrosion reaction on the electrode surface (for example, iron phosphates) involving inhibitor molecules and their reactive products [21,22].The diameters of capacitive loops increase with the increase in MTTT concentration, which indicates the increase of charge transfer resistance and improvement in inhibiting effect on carbon steel corrosion. It can be observed that the shapes of the impedance plots for the inhibited electrodes are not essentially different from those of the uninhibited electrodes.

The table 2 shows that the presence of MTTT in 2 M H_3PO_4 solutions increases the charge transfer impedance due to the formation of protection layer on the steel surface, but it does not change other aspects of the corrosion behavior. The CPE impedance is defined by two values, Q and n and is described by the equation [23,24]:

$$Z_{CPE} = Q^{-1}(i\,\omega)^{-\alpha} \qquad (3)$$

Where Q is the CPE constant, ω is the angular frequency (in rad.s^{-1}), such as $i^2 = -1$ is the imaginary number and n is a CPE exponent which can be employed as a gauge of the heterogeneity or roughness of the surface [25,26]. The CPE comportment can be quantified by plotting the imaginary part of the impedance versus frequency in logarithmic coordinate. The double layer capacitance (C_{dl}) in the present study was calculated using the following relation:

$$C_{dl} = (Q \times R_{ct}^{1-\alpha})^{1/\alpha} \qquad (4)$$

Table 2: Electrochemical impedance measurements for carbon steel immersed in 1M HCl in absence and presence different concentrations of MTTT at 303K.

Concentration (M)	R_s ($\Omega.cm^2$)	R_1 ($\Omega.cm^2$)	R_2 ($\Omega.cm^2$)	Rct ($\Omega.cm^2$)	$10^4 Q$ ($\Omega S^n cm^2$)	n	L (H cm^2)	C_{dl} ($\mu F.cm^{-2}$)	η_{EIS} %
Blank	2.841	2.821	0.5807	3.4017	5,364	0,8788	0.01693	224,783	-
10^{-6}	4.25	8.437	0.7971	9.2340	4,681	0,8799	0.78301	222,655	63.16
10^{-5}	4.763	20.02	1.0090	21.029	3,520	0,8801	2.10904	180,416	83.82
10^{-4}	3.975	28.68	7.4670	36.147	2,537	0,8891	3.50110	141,307	90.58
10^{-3}	2.666	70.42	14.13	84,550	1,628	0,8899	4.66600	95,8030	95.97

The table 2 clearly shows that in the whole concentration range, the charge transfer resistance Rct increases with MTTT concentration, hence better inhibition power is achieved. This effect is connected with simultaneous decrease of the double-layer capacitance (C_{dl}), often observed when adsorption of organic molecules on electrode surfaces takes place [27].

Indeed, the values of surface heterogeneity were exponent n ($0 \leq n \leq 1$) [28].the increase of the n value after addition of MTTT in 2 M H_3PO_4 solution (0,8799–0,8899) when compared to that obtained in uninhibited solution (0,8788) can be explained by some decrease of the initial surface heterogeneity, due to the adsorption of the inhibitor on the most active adsorption sites on the steel surface[29]. At LF region, the inductance (L) increases with MTTT concentration. The η_{EIS}% obtained from EIS techniques and those calculated from polarization curves measurements are in good agreements in all compounds.

2.3. Effect of temperature

The effect of temperature on the corrosion inhibition property of the MTTT, was studied through Potentiodynamic polarization experiments were conducted in the range of 303–333 K, in the absence and presence of 10^{-3} M of inhibitor during 30 min of immersion. The analysis of the obtained data, presented in Table 3 and illustrated in Fig. 5, shows a rise of corrosion current density (I_{corr}) with the increase of temperature and it is more pronounced for uninhibited solution (2 M H_3PO_4).
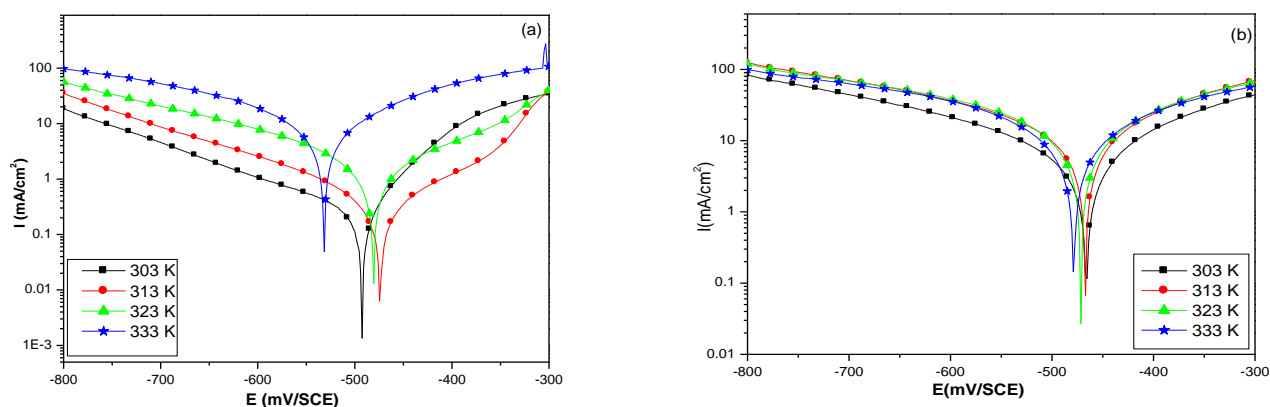
Figure 5: Polarization curves of carbon steel in 2M $H_3PO_4$with (a) and without (b) 10^{-3} M of MTTTfor various temperatures

Table 3: Temperature influence on the Potentiodynamic polarization parameters for carbon steel in 2M H_3PO_4 with and without 10^{-3} M of MTTT.

	Temperature (K)	E_{corr} (mVvs.SCE)	I_{corr} (µA cm^2)	$-\beta_c$ (mVdec^{-1})	η_{Tafel} (%)
Blank	303	-470	3405	193	-
	313	-470	5121	112	-
	323	476	6398	140	-
	333	483	8871	191	-
MTTT	303	-496	271	179	92.04
	313	476	578	192	88,71314
	323	485	1230	152	80,77524
	333	536	6460	153	27,17845

These results show that the inhibition efficiency depends on the temperature and decreases with the rise of temperature, indicating that higher temperature dissolution of carbon steel predominates on adsorption of MTTT at the metal surface. This can be explained by the decrease of the adsorption process at high temperature, and can suggest a physical adsorption mode. In order to calculate activation thermodynamic parameters of the corrosion process, Arrhenius Eq. (5) and transition state Eq. (6) were used [30]:

$$i_{corr} = A \exp\left(-\frac{E_a}{RT}\right) \qquad (5)$$

$$i_{corr} = \frac{RT}{Nh} \exp\left(\frac{\Delta S_a}{R}\right) \exp\left(-\frac{\Delta H_a}{RT}\right) \qquad (6)$$

Where E_a is the apparent activation corrosion energy, R is the universal gas constant, A is the Arrhenius pre-exponential factor, h is Plank's constant, N is Avogadro's number, ΔS_a is the entropy of activation and ΔH_a is the enthalpy of activation. The figure 6 present Arrhenius plots for the corrosion rate of carbon steel. Values of apparent activation energy of corrosion (E_a) in the absence and the presence of MTTT, were determined from the slope of $\ln(I_{corr})$ vs. 1/T plots and given in Table 4.
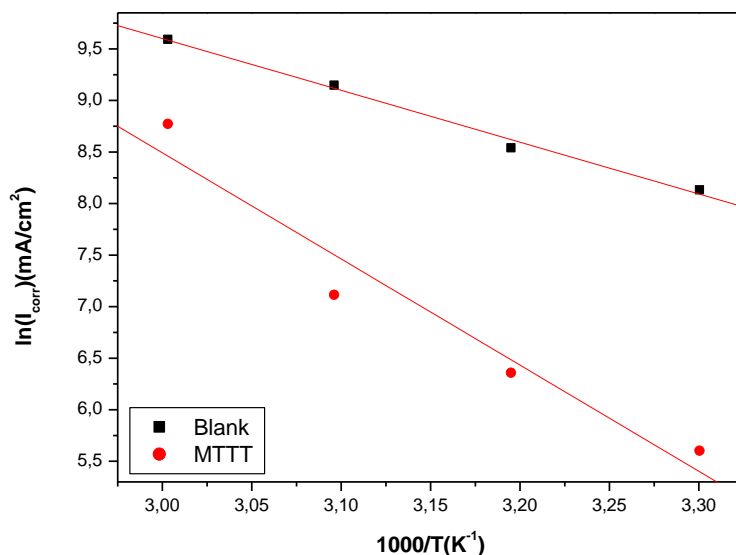
Figure 6: Arrhenius plots for carbon steel corrosion current density (I_{corr}) in 2M H_3PO_4 in absence and in presence of 10^{-3}M of MTTT.
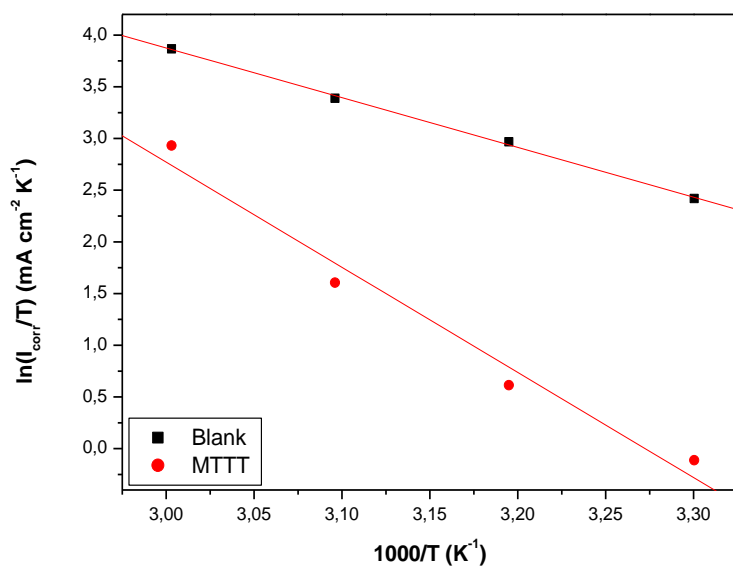
Figure 7: Transition-state plots for carbon steel current density (I_{corr}) in 2M H_3PO_4 inabsence and in presence of 10^{-3} M of MTTT.

Table 4: Corrosion kinetic parameters for carbon steel in 2M H_3PO_4 in absence and presenceof 10^{-3}M of MTTT.

Inhibitor (M)	E_a(Kj mol^{-1})	ΔH_a(kJ mol^{-1})	ΔS_a (J mol^{-1} K^{-1})
Blank	41.73	34,752	-45,394
MTTT	83.14	84,553	79,149

The table 4 shows that the E_a in presence of inhibitor increase when compared to that in its absence may be interpreted as physical adsorption [31]. Szauer et al. explained that the increase in activation energy can be attributed to an appreciable decrease in the adsorption of the inhibitor on the steel surface with increase in temperature [32]. As adsorption decreases more desorption of inhibitor molecules occurs because these two opposite processes are in equilibrium. Due to more desorption of inhibitor molecules at higher temperatures the greater surface area of steel comes in contact with aggressive environment, resulting increased corrosion rates with increase in temperature [33]. Other researchers explained that the rise of activation energy can be explained by decrease in the adsorption of the inhibitor on the steel surface with increase in temperature [32].

Fig. 7 shows a plot of ln (I_{corr}/T) against 1/T. Straight lines are obtained with a slope of (ΔH_a/R) and an intercept of (ln R/Nh + ΔS_a/R) from which the values of ΔH_a and ΔS_a are calculated and are listed in Table 3. Inspection of these data reveals that the ΔH_a value for dissolution reaction of carbon steel is higher in the presence of MTTT (84.553 kJmol1) than that in its absence (34.752 kJmol1). The positive signs of ΔH_a reflect the endothermic nature of the carbon steel dissolution process suggesting that its dissolution is slow in the presence of MTTT. It is clear from Table 3 that the value of entropy of activation (ΔS_a) in presence of MTTT is higher compared with uninhibited solution. Generally, the increase of ΔS_a can be interpreted as an increase in disorder as the reactants are converted to the activated complexes.

2.4. Adsorption isotherm and thermodynamic parameters

Adsorption isotherms are usually used to describe the adsorption process. The most frequently used isotherms include: Langmuir, Frumkin, Temkin. The establishment of adsorption isotherms that describe the adsorption of a corrosion inhibitor can provide important clues to the nature of the metal–inhibitor interaction. Adsorption of the organic molecules occurs as the interaction energy between molecule and metal surface is higher than that between the water molecule and the metal surface [34]. In order to obtain the adsorption isotherm, the degree of surface coverage (θ) for various concentrations of the MTTT has been calculated at 303 K from the Potentiodynamic polarization measurements by the ration η_{Taf}(%)/100. The results obtained for MTTT in 2 M H_3PO_4 solution fit well Langmuir adsorption isotherm given by Eq. (7) [35]:

$$\frac{C_{inh}}{\theta} = C_{inh} + \frac{1}{K_{ads}} \qquad (7)$$

Where θ is the degree of surface coverage and $C_{inh}$is the inhibitor concentration in the electrolyte. K_{ads} is the equilibrium constant of the adsorption process and is related to the standard Gibbs energy of adsorption ΔG_{ads}°, according to [36]:

$$K_{ads} = \frac{1}{55.55} \exp(-\frac{\Delta G_{ads}^{\circ}}{RT}) \qquad (8)$$

Where R is the universal gas constant and T is the absolute temperature. The value 55.5 in the above equation is the concentration of water in solution in mol/l.

The experimental (points) and calculated isotherms (lines) are plotted in Fig. 8. A very good fit is observed with the regression coefficient up to 0.99 and the obtained line has slopes very close to unity, which suggests that the experimental data are well described by Langmuir isotherm. This kind of isotherm involves the assumption of no interaction between the adsorbed species on the electrode surface [37]. The calculated ΔG_{ads} value, using Eq. (7), is 30.708 kJ mol^{-1}. Generally speaking, the adsorption type is regarded as physisorption if the absolute value of ΔG_{ads} was of the order of 20 kJ mol^{-1} or lower. The inhibition behavior is attributed to the electrostatic interaction between the organic molecules and iron atom. When the absolute value of ΔG_{ads} is of the order of 40 kJ mol^{-1} or higher, the adsorption could be seen as chemisorption. Based on the literature and the activation

results [38], the calculated ΔG_{ads} values in this work indicate that the adsorption mechanism of MTTT on carbon steel in 2 M H_3PO_4 solution at 303 K is mainly electrostatic-adsorption (ionic) [39].
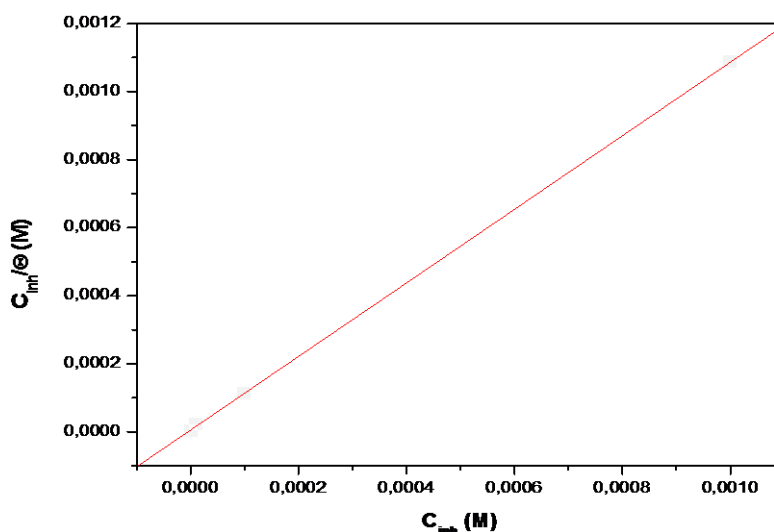
Figure 8: Langmuir isotherm adsorption model of MTTT on the carbon steel surface in2M H_3PO_4.

Conclusion:

The MTTT good excellent inhibition properties for the corrosion of carbon steel in 2M H_3PO_4 at 303 K, and the inhibition efficiency, η(%), increases with increase in the inhibitor concentration. The η(%) of MTTT decrease proportionally with increasing temperature (303–333K) and its addition to 2 M H_3PO_4 leads to increase of apparent activation energy (E_a) of corrosion process. The corrosion process is inhibited by the adsorption of MTTT on steel surface and the adsorption of the inhibitor fits a Langmuir isotherm model at 303 K. The calculated value of ΔG_{ads} reveals that the adsorption mechanism of MTTT on carbon steel surface in 2 M H_3PO_4 solution is mainly electrostatic-adsorption. Based on the Tafel polarization results, MTTT can be classified as mixed inhibitor. The EIS spectra are well described by the proposed structural models. Polarization and EIS methods are in good agreement.

References

1. Zakaria K., Negm N.A., Khamis E.A., Badr E.A., *Chem. Eng*. 61(2016) 316.
2. Avdeev Y.G., Kuznetsov Y.I.,Buryak A.K., *Corros. Sci.* 69 (2013) 50.
3. Raja P.B., Qureshi A.K.,Rahim A.A., Osman H., Awang K., *Corros. Sci*. 69 (2013) 292.
4. RevieR.W., Uhlıgısı,*Corrosion Handbook*, third ed., Wiley, New Jersey (2011).
5. Hegazy M.A., Aiad I., *J. Ind. Eng. Chem.*31(2015)91.
6. Aliofkhazraei M., *Developments in Corrosion Protection, InTech*, ISBN 978-953-51-1223-5 (2014).
7. Hooshm A.S., Sharifi M., Zaarei D., Shishesaz M.R., *J. Environ. Chem. Eng*. 1 (2013) 652.
8. Bouklah, M., Ouassini, A., Hammouti, B., El Idrissi, A., *Appl. Surf. Sci.,* 250 (2005) 50-56.
9. Finsgar M., Jackson J., *Corros. Sci.* 86 (2014) 17.
10. El Issami S., Bazzi L., Mihit M., Hammouti B., Kertit S., Addi E.A., Salghi R., *Pigment and Resin Technology,* 36 (2007) 161-168
11. Dabholkar V.V., More *G.D., Indian J. Chem.* 43 (2004) 682.
12. Essassi E.M., Lavergne J.P., Viallefont P., *J. Heterocycl. Chem.* 13 (1976) 885.
13. Essassi E.M., Lavergne J.P., Viallffont P., *Tetrahedron*, 33 (1977) 2807.
14. Farrugia L.J. *J. Appl. Cryst*. 45 (2012) 849.
15. Gupta M., Paul S., Gupta R. *Eur. J. Med. Chem.* 46 (2011) 631.

16. El Bakri Y., Harmaoui A., Essassi E. M., Saadi M., El Ammari L*., IUCr Data* .1, x161229 (2016).
17. Zarrok H., Zarrouk A., Hammouti B., Salghi R., Jama C., Bentiss F., *Corros. Sci.* 64 (2012) 243.
18. EL Aoufir Y., Lgaz H., Bourazmi H., Kerroum Y., Ramli Y., Guenbour A., Salghi R., El-Hajjaji F., Hammouti B., Oudda H., *J. Mater. Environ. Sci.* 7 (12) (2016) 4330.
19. Gojic M., *Corros. Sci.* 43 (2001) 919.
20. El Ouali I., Hammouti B., Aouniti A., Ramli Y., Azougagh M., Essassi E.M., Bouachrine M., *J. Mater. Environ. Sci.* 1 N°1 (2010) 1 - 8..
21. Li P., Li J.Y., Tan K.L., Lee J.Y., *Electrochim. Acta* 42 (1997) 605.
22. Labjar N., Lebrini M., Bentiss F., Jama C., El Hajjaji S., Chihib N.E., *Mater. Chem. Phys*. 119 (2010) 330.
23. Stoynov Z., *Electrochim. Acta,* 35 (1990) 1493.
24. Macdonald J.R., *J. Electroanal. Chem.* 223 (1987) 25.
25. Li P., Lin J.Y., Tan K.L., Lee J.Y., *Electrochim. Acta.* 42 (1997) 605.
26. Lopez D.A., Simison S.N., De Sanchez S.R., *Electrochim. Acta*. 48 (2003) 845.
27. Outirite M., Lagrenée M., Lebrini M., Traisnel M., Jama C., Vezin H., Bentiss F., *Electrochim. Acta* 55 (2010) 1670.
28. Lopez D.A., Simison S.N., Sanchez S.R., *Electrochim. Acta* 48 (2003) 845.
29. Growcock F.B., Jasinski J.H., *J. Electrochem. Soc.* 136 (1989) 2310.
30. Bockris J.O.M., Reddy A.K.N., *Modern Electrochemistry*, vol. 2, Plenum Press, New York, (1977).
31. Quraishi M.A., Jamal D., *Mater. Chem. Phys*. 68 (2001) 283.
32. Benabdellah M., Tounsi A., Khaled K.F., Hammouti B., *Arabian Journal of Chemistry* 4 (2011) 17-24
33. Wang H.L., Fan H.B., Zheng J.S., *Mater. Chem. Phys*. 77 (2003) 655.
34. Moretti G., Quartarone G., Tassan A., Zingales A., *Mater. Corros.* 45 (1994) 641.
35. Döner A., Solmaz G., Özcan M., Kardas G., *Corros. Sci.* 53 (2011) 2902.
36. Flis J., Zakroczymski T., *J. Electrochem. Soc*. 143 (1996) 2458.
37. Elayyachy M., El Idrissi A., Hammouti B., *Corros. Sci*. 48 (2006) 2470.
38. Hammouti B., Zarrouk A., Al-Deyab S.S., Warad I., *Oriental Journal of Chemistry* 27 (2011) 23-31
39. Ali. S.A., Al-Muallem H.A., Saeed M.T., Rahman S.U., *Corros. Sci*. 50 (2008) 664.

(2017) ; http://www.jmaterenvironsci.com